

Diffractive heavy quarkonium photoproduction and electroproduction in QCD

Leonid Frankfurt*

School of Physics and Astronomy, Raymond and Beverly Sackler Faculty of Exact Sciences, Tel Aviv University, Tel Aviv, Israel

Werner Koepf†

Department of Physics, The Ohio State University, Columbus, Ohio 43210

Mark Strikman‡

Department of Physics, Pennsylvania State University, University Park, Pennsylvania 16802

(Received 5 February 1997; published 5 December 1997)

Hard diffractive photoproduction and electroproduction of heavy vector mesons (J/ψ and Y) is evaluated within the leading $\alpha_s \ln(Q^2/\Lambda_{\text{QCD}}^2)$ approximation of QCD. Different from our earlier work on that subject, also the production of transversely polarized vector mesons is calculated. Special emphasis is placed on the role of the vector meson's $q\bar{q}$ light-cone wave function. In that context, conventional nonrelativistic quarkonium models and a light-front QCD bound state calculation are critically examined and confronted with QCD expectations. Our numerical analysis finds a significant high momentum tail in the latter wave functions and a deviation from the expected asymptotic behavior of $\phi_V(z, b=0) \propto z(1-z)$. We then design an interpolation to match the quarkonium models at large interquark separations with QCD expectations at small distances. We use these results to compare our predictions for the forward differential cross section of J/ψ photoproduction and electroproduction with recent experimental results from DESY HERA. In addition, our earlier discussion of ρ^0 electroproduction is updated in light of recent experimental and theoretical enhancements. [S0556-2821(98)05601-X]

PACS number(s): 13.85.Ni, 12.38.Bx, 12.39.Jh, 12.39.Ki

I. INTRODUCTION

Diffractive vector meson production opens a precious window on the interface between perturbative QCD and hadronic physics. While elastic processes are commonly described through nonperturbative, phenomenological methods, such as, for instance, soft Pomeron exchange [1], hard inclusive reactions—most prominently deep inelastic lepton scattering—are, in a sense, exactly calculable as a consequence of the QCD factorization theorem. These two classes of processes now meet at the DESY ep collider HERA. However, similar to inclusive deep inelastic scattering, also the amplitude for diffractive (coherent) production of vector mesons in deep inelastic lepton-nucleon scattering factorizes into a hard part calculable in perturbative QCD ($p\text{QCD}$) convoluted with the nonperturbative off-diagonal gluon distribution in the target [2]. A rigorous QCD-based proof of the factorization theorem for hard exclusive electroproduction of vector mesons, valid to all orders in perturbation theory, was recently given in Ref. [3]. This theorem holds if only short distances contribute, which is the case for the production of longitudinally polarized ρ^0 at sufficiently large Q^2 or heavy flavor photo- and electroproduction [4].

For large but nonasymptotic photon virtuality, the hard amplitude for exclusive vector meson production is sensitive to the transverse momentum distribution in the light-cone

wave function of the $q\bar{q}$ leading Fock component of the produced vector meson [4]. This leads to a suppression of the asymptotic amplitude, i.e., to an interplay between the quark(antiquark) momentum distribution in the vector meson and the Q^2 dependence of the corresponding cross section. That, in turn, allows to extract information on this wave function—and hence on the three dimensional distribution of color in the produced hadron—from the Q^2 and the t dependences of the cross section.

In this work, we focus the QCD analysis of Refs. [2] and [4] on heavy quarkonium (J/ψ and Y) photoproduction and electroproduction. Furthermore, we extend the respective formalism, which in Refs. [2] and [4] was applied to the production of longitudinally polarized vector mesons only, to transverse polarizations as well. The important role the vector meson's $q\bar{q}$ light-cone wave function plays in diffractive photoproduction and electroproduction at nonasymptotic Q^2 requires a detailed study of this quantity. Motivated by the large value of the quark mass in heavy quarkonia, we start from conventional nonrelativistic potential models [5–8] and/or a nonrelativistic light-front QCD bound state calculation [9]. We then critically examine the respective wave functions and confront them with QCD expectations.

In particular for the J/ψ meson, our numerical analysis yields a significant value for the high momentum component in the respective nonrelativistic wave functions $\phi_V(k)$. For instance for the potential model of Ref. [5], the region $v/c \geq 1$, where the nonrelativistic approximation is definitely inadequate, contributes over 30% to the integral $\int d^3k \phi_V(k)$. Latter integral appears in the expression for the $V \rightarrow e^+e^-$ decay width. This is illustrated in Fig. 6, and it is in line with

*On leave of absence from the St. Petersburg Nuclear Physics Institute, Russia.

†Now at NeuralWare, a subsidiary of Aspen Technology Inc.

‡Also at St. Petersburg Nuclear Physics Institute, Russia.

the QCD prediction of large relativistic corrections to the corresponding bound state equations [10]. Those large relativistic effects put the validity of a nonrelativistic description of J/ψ mesons—and, in particular, a nonrelativistic evaluation of their production in high energy processes—seriously into question. Our analysis shows that the Q^2 dependence of J/ψ electroproduction, the photoproduction cross section ratios of Y and J/ψ mesons, and modifications in the t slope of those cross sections are good probes for the color distribution in the light-cone wave function of the vector mesons as well as the dependence of the parton distribution in the target on the produced meson's transverse size. In particular, these effects lead to an enhancement of the cross section ratio for diffractive electroproduction of Y and J/ψ mesons by a factor ≈ 10 for the same x as compared to the naive scaling estimate. This was discussed already in Ref. [4].

In addition, if we express the nonrelativistic wave functions in terms of light-cone coordinates, we find that they do not display the expected asymptotic behavior [11] $\int d^2k_t \phi_{VL}(z, k_t) \propto z(1-z)$ in the vicinity of $z=0$ or $z=1$. This is illustrated in Fig. 8. Another mismatch between the nonrelativistic and the light-cone approach appears within the evaluation of the $V \rightarrow e^+e^-$ decay width. When $\Gamma_{V \rightarrow e^+e^-}$ is calculated from the nonrelativistic wave function $\phi_V(k)$, a QCD correction factor, $1 - 16\alpha_s/3\pi$, appears [12], which can be numerically large [$16\alpha_s/3\pi \approx 0.5$ for J/ψ where we use $\alpha_s(J/\psi) = 0.3$] while no such term is present in the relation [13] with the light-cone $q\bar{q}$ wave function $\phi_V(z, k_t)$. This difference may be important in practice since the Schwinger formula for the positronium decay [14] becomes inaccurate for charmonium where the high momentum component in the wave function is not small. To remedy these deficiencies, we designed an interpolation for the wave function of heavy quarkonia which smoothly matches the wave functions obtained at average interquark separations from nonrelativistic potential models (or within a light-front QCD bound state calculation) with QCD predictions at small distances.

The basic difference of the current work from Ref. [4] is that the formulas valid in leading order in $1/(Q^2 + 4m^2)$ are derived by decomposing Feynman diagrams over the *transverse* distance between bare quarks, and that the quarkonium light-cone wave functions which we used respect QCD predictions for their high momentum tail. As for any hard process, the cross section is expressed through the distribution of bare quarks in the vector meson and not through the distribution of constituent quarks, as it has been assumed in Refs. [15] and [16]. In the latter investigations, the cross section for diffractive photoproduction and electroproduction of J/ψ mesons was evaluated in the Balitskii-Fadin-Kuraev-Lipatov (BFKL) approximation and while employing a nonrelativistic constituent quark model. No corrections arising from the quark motion within the produced J/ψ mesons were considered in Ref. [15]. In a later work [16], the authors then argued that the respective corrections are small within realistic charmonium models. This is at variance with our findings. In addition, our numerical analysis shows that the static approximation used in Refs. [15] and [16] is not in line with conventional charmonium models. Neglect of quark Fermi motion and related color screening effects in Refs. [15,16] leads to factor ≈ 3 suppression for the ratio of cross sections

of photoproduction of Y versus J/ψ mesons as compared to the results in this paper.

After outlining the basic formalism in Sec. II, in Sec. III, we discuss the heavy vector meson's light-cone wave function which describes its leading $q\bar{q}$ Fock state component. We then compare, in Sec. IV, with recent experimental results from HERA for J/ψ photoproduction [17] and electroproduction [18]. In Sec. V, we update our discussion of ρ^0 electroproduction in light of recent experimental [19] and theoretical [20] enhancements. We summarize and conclude in Sec. VI.

II. THE BASIC FORMALISM

A. The forward differential cross section

In Ref. [2], the forward differential cross section for the production of longitudinally polarized vector mesons was deduced within the double logarithmic approximation, i.e., $\alpha_s \ln(Q^2/\Lambda_{\text{QCD}}^2) \ln(1/x) \sim 1$, with the result of

$$\left. \frac{d\sigma_{\gamma^* N \rightarrow VN}}{dt} \right|_{t=0} = \frac{4\pi^3 \Gamma_V M_V}{3\alpha_{EM} Q^6} \eta_V^2 | \alpha_s(Q^2) \times (1 + i\beta)x G_N(x, Q^2) |^2. \quad (1)$$

Here, Γ_V stands for the decay width of the vector meson into an e^+e^- pair, $\beta = \text{Re}_A/\text{Im}_A \approx (\pi/2)\partial \ln[\text{Im}A]/\partial \ln x$ is the relative contribution of the amplitude's real part, and the leading twist correction

$$\eta_V \equiv \frac{1}{2} \frac{\int [dz/z(1-z)] \int d^2k_t \phi_V(z, k_t)}{\int dz \int d^2k_t \phi_V(z, k_t)}, \quad (2)$$

accounts for the difference between the vector meson's decay into an e^+e^- pair and diffractive vector meson production. Here $\phi_V(z, k_t)$ is the wave function of the longitudinally polarized vector meson. We implicitly use the light-cone gauge which provides for an unambiguous separation of the k_t dependence of the meson (photon) wave function and gluon degrees of freedom. Note that the original formula deduced in Ref. [2] lacks a factor of 4. This misprint has been corrected in Ref. [4]. In Ref. [4], it was shown that the formula in Eq. (1) is valid also within the more conventional leading $\alpha_s \ln(Q^2/\Lambda_{\text{QCD}}^2)$ approximation. Although, in principle, hard diffractive processes are expressed in terms of nondiagonal parton densities, a recent analysis [21] of the QCD evolution equations for nondiagonal parton distributions at small x shows that the gluon nondiagonal parton distributions are close to though somewhat larger than the diagonal gluon distributions in the kinematic region discussed in this paper. This difference weakly depends on x and slowly increases with increase of Q^2 . In particular, for the case of J/ψ production at $x \leq 10^{-2}$ this effect leads to renormalization of the photoproduction cross section by a factor ~ 1.4 . Numerical study of these effects for ρ and J/ψ production will be presented elsewhere.

In Ref. [4], also next-to-leading order (NLO) as well as higher twist corrections were introduced. First, it was argued that the strong coupling constant and the nucleon's gluon density have to be evaluated not at Q^2 but at a Q_{eff}^2 . This is due to the so-called ‘‘rescaling of hard processes’’ which will be discussed in more depth later. And, secondly, a suppression factor $T(Q^2)$ was deduced which measures the deviation of the cross section from its asymptotic prediction in

Eq. (1), and which stems from the transverse Fermi motion of the quarks in the produced vector meson. This yields [4]

$$\left. \frac{d\sigma_{\gamma^* N \rightarrow VN}}{dt} \right|_{t=0} = \frac{4\pi^3 \Gamma_V M_V}{3\alpha_{EM} Q^6} \eta_V^2 T(Q^2) |\alpha_s(Q_{\text{eff}}^2)|^2 \times (1+i\beta)x G_N(x, Q_{\text{eff}}^2)^2, \quad (3)$$

with the correction factor

$$T(Q^2) = \left[\frac{(Q^4/4) \int dz \int d^2k_t \phi_V(z, k_t) \Delta_t \phi_\gamma(z, k_t)}{\int [dz/z(1-z)] \int d^2k_t \phi_V(z, k_t)} \right]^2, \quad (4)$$

where

$$\phi_\gamma(z, k_t) = \frac{1}{Q^2 + (k_t^2 + m^2)/z(1-z)} \quad (5)$$

is the photon's $q\bar{q}$ light-cone wave function, Δ_t is the transverse Laplacian $\Delta_t = \Sigma(d/dk_t)^2$, and where, for the production of light mesons, the current quark mass was set to zero.

In this investigation, we focus on the photoproduction and electroproduction of heavy quarkonium (J/ψ and Υ), and we extend the respective formalism to the production of transversely polarized heavy vector mesons as well. Note that, for sufficiently heavy quark mass, the applicability of the QCD factorization theorem to the diffractive photoproduction of transversely polarized vector mesons can be justified because the transverse size of quarkonium decreases with the mass of the heavy quarks. The result for the forward differential cross section for photoproduction and electroproduction of heavy vector mesons, which will be deduced in detail in the following, is

$$\left. \frac{d\sigma_{\gamma^{(*)} N \rightarrow VN}}{dt} \right|_{t=0} = \frac{4\pi^3 \Gamma_V M_V^3}{3\alpha_{EM} (Q^2 + 4m^2)^4} \eta_V^2 T(Q^2) |\alpha_s(Q_{\text{eff}}^2)|^2 (1+i\beta)x G_N \times (x, Q_{\text{eff}}^2)^2 \left(R(Q^2) + \epsilon \frac{Q^2}{M_V^2} \right). \quad (6)$$

Here, η_V is again the leading twist correction of Eq. (2), the factor $T(Q^2)$, which was introduced in Ref. [4], accounts for effects related to the quark motion in the produced vector meson, and $\epsilon = (1-y)/(1-y+y^2/2)$ is a parameter related to the (virtual) photon's polarization. Here, y is the energy fraction (in the target rest frame) transferred from the scattered lepton to the target. A value of $\epsilon=0$ corresponds to purely transverse polarization—which is always the case for real photons, i.e., $Q^2=0$ —and $\epsilon=1$ refers to an equal mix of longitudinal and transverse polarizations. The latter is typical for HERA kinematics at large Q^2 . The factor $R(Q^2)$ parametrizes the relative contribution of the production of transversely polarized vector mesons as compared to the naive prediction, i.e., $\sigma_T/\sigma_L = R(Q^2)(M_V^2/Q^2)$ instead of simply $\sigma_T/\sigma_L = M_V^2/Q^2$.

Different from Ref. [4], the current quark mass was not set to zero, i.e., we kept leading powers over $1/(Q^2 + 4m^2)$ and not just $1/Q^2$. This, in turn, yields for the correction factors $T(Q^2)$ and $R(Q^2)$:

$$T(Q^2) = \left[\frac{(Q^2 + 4m^2)^2 \int dz \int d^2k_t \phi_V(z, k_t) \Delta_t \phi_\gamma(z, k_t)}{4 \int [dz/z(1-z)] \int d^2k_t \phi_V(z, k_t)} \right]^2, \quad (7)$$

$R(Q^2)$

$$= \left[\frac{m^2 \int [dz/z^2(1-z)^2] \int d^2k_t \phi_V(z, k_t) \Delta_t \phi_\gamma(z, k_t)}{4M_V^2 \int dz \int d^2k_t \phi_V(z, k_t) \Delta_t \phi_\gamma(z, k_t)} \right]^2, \quad (8)$$

where we employed again $\phi_\gamma(z, k_t)$ of Eq. (5).

The $T(Q^2)$ and $R(Q^2)$ displayed in the above constitute one of our main original new results. These formulas are derived by building a decomposition over the transverse distance between the bare quarks, i.e., over powers of $1/(Q^2 + 4m^2)$. However, some caution is necessary at this point. The accuracy of this approximation for the calculation of R at $Q^2 \gg M_V^2$ can be questioned because of an enhancement of end point ($z=0$ and $z=1$) contributions at large Q^2 . But in these kinematics, the production of longitudinally polarized vector meson would dominate [2]. In order to be able to evaluate the correction factors of Eqs. (7) and (8), we need the light-cone wave function of the $q\bar{q}$ leading Fock state in the vector meson. We will discuss this quantity in detail in the next section.

Our master formula in Eq. (6) yields a few fundamental predictions: (1) the cross sections raise with energy very rapidly due to the presence of the gluon density which increases fast at small x , (2) the t slope is expected to be almost the same for all hard diffractive processes of the kind studied here,¹ and (3) the production of longitudinally polarized vector mesons will dominate at large Q^2 . Note, also, that this is only a leading order analysis, and to achieve a nonambiguous interpretation of the processes considered here it would be necessary to evaluate also more accurately NLO corrections as well as the higher twist the contribution of the $|q\bar{q}G\rangle$ component in the light-cone wave functions of the photon and the produced vector meson.

B. The color-dipole cross section

As discussed at length in Refs. [2], [3], and [4], due to the QCD factorization theorem and the large longitudinal coherence length, $l_c \approx 1/2m_N x$, associated with high energy (small x) diffractive processes, in leading order in $\alpha_s \ln(Q^2/\Lambda_{\text{QCD}}^2)$, the amplitude for hard diffractive vector meson production off a nucleon, depicted in Fig. 1, can be written as a product of three factors:

$$\mathcal{A}_{\gamma^* N \rightarrow VN} \propto \Psi(\gamma^* \rightarrow q\bar{q}) \cdot \sigma_{q\bar{q}N} \cdot \Psi(q\bar{q} \rightarrow V), \quad (9)$$

where $\Psi(\gamma^{(*)} \rightarrow q\bar{q})$ is the light-cone wave function for a photon to split into a $q\bar{q}$ pair, $\sigma_{q\bar{q}N}$ is the interaction cross section of the $q\bar{q}$ pair with the target nucleon, and

¹This is because the t slope in the hard vertex scales like the maximum of the mass of the heavy quark and Q^2 .

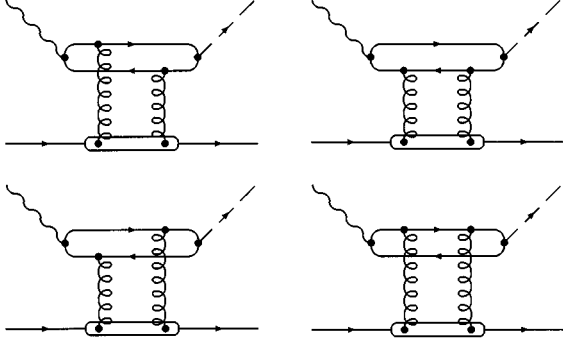


FIG. 1. Feynman diagrams relevant for the evaluation of the amplitude for diffractive production of vector mesons, i.e., the $\gamma^{(*)} + N \rightarrow V + N$ process, in leading $\alpha_s \ln(Q^2/\Lambda_{\text{QCD}}^2)$ approximation.

$\Psi(q\bar{q} \rightarrow V)$ is the amplitude for the $q\bar{q}$ pair to transform into the vector meson V in the exit channel.

As was shown in Ref. [4], for sufficiently large Q^2 and longitudinal polarization, the above process is dominated by $q\bar{q}$ configurations where the quark and antiquark are separated by a small transverse distance b . Then, $\sigma_{q\bar{q}N}$ is the color-dipole cross section [22,23]

$$\begin{aligned} \sigma_{q\bar{q}N}(x, b) &= \frac{\pi^2}{3} b^2 [\alpha_s(Q_{\text{eff}}^2) x G_N(x, Q_{\text{eff}}^2)]_{x=(Q^2+M_V^2)/s, Q_{\text{eff}}^2=\lambda/b^2}. \end{aligned} \quad (10)$$

Qualitatively, Eq. (10) can be understood in the following way: The four diagrams of Fig. 1 lead to an expression in the amplitude of the form

$$\sigma_{\gamma^*N} [2\phi_\gamma(z, k_t) - \phi_\gamma(z, k_t + l_t) - \phi_\gamma(z, k_t - l_t)], \quad (11)$$

where the Sudakov variable z denotes the fraction of the photon's momentum carried by one of the quarks, $\pm k_t$ is their transverse momentum, and l_t is the gluons' transverse momentum. For small l_t , this yields

$$\sigma_{\gamma^*N}. \quad (12)$$

Via Fourier transform into the transverse impact parameter space and after pulling out the wave function of the γ^* , we obtain

$$\sigma_{q\bar{q}N} \propto b^2. \quad (13)$$

The gluon density xG_N arises as the diagrams in Fig. 1 represent not simple two-gluon exchange but rather the coupling to the full nonperturbative gluon ladder. For further details see Ref. [24] where the quantity $\sigma_{q\bar{q}N}$ was derived rigorously. In the following, we will show that—due to the large value of the current quark mass—the dominance of short distances holds for diffractive production of heavy flavors also for $Q^2=0$ and both for longitudinal as well as transverse polarizations.

Note that, due to the difference in the invariant mass between the photon and the vector meson, the light-cone momentum fractions of the gluons in the initial and final state,

β_i and β_f , are not the same, and therefore, in principle, an off-diagonal gluon distribution should enter into Eqs. (6) and (10). This was first recognized in Ref. [4], and then elaborated on in Refs. [25], [26], and [21]. A simple kinematical consideration yields $\beta_i \approx [(M_X^2 + \langle l_t^2 \rangle + Q^2)/(Q^2 + M_V^2)]x$ and $\beta_f \approx [(M_X^2 + \langle l_t^2 \rangle - M_V^2)/(Q^2 + M_V^2)]x$, where $\langle l_t^2 \rangle$ is the average transverse momentum of the exchanged gluons and $M_X^2 = \langle (k_t^2 + m^2)/z(1-z) \rangle$ is the invariant squared mass of the produced $q\bar{q}$ pair. Within the $\alpha_s \ln(Q^2/\Lambda_{\text{QCD}}^2)$ approximation, the nondiagonal gluon distribution is shown [21] to be not far—from the small x that are important experimentally—from the diagonal one. This is because, within this approximation, the appropriate energy denominators only weakly depend on β_i .

C. Rescaling of hard processes

As outlined in detail in Ref. [4], the parameter λ , which fixes the scale in the gluon density and the strong coupling in Eqs. (6) and (10), is determined by comparison with the longitudinal structure function $F_L(x, Q^2) \propto y G_N(y, Q^2)|_{y \approx 2.5x}$, i.e., by setting

$$y G_N(y, Q^2)|_{y \approx 2.5x} \propto \int d^2 b d z |\phi_{\gamma_L^*}(z, b)|^2 \sigma_{q\bar{q}N}(2.5x, b), \quad (14)$$

where

$$\phi_{\gamma_L^*}(z, b) = 2Qz(1-z)K_0[b\sqrt{Q^2(1-z)+m^2}] \quad (15)$$

is the light-cone wave function of the $q\bar{q}$ leading Fock component in a longitudinally polarized virtual photon, and m is the current quark mass, which was set to zero when we evaluated Eq. (14) (since the contribution of charm quarks to F_L is small in the considered kinematics). In Eqs. (14) and (15), b is the transverse distance between the quark and antiquark within the photon. The quantity λ is adjusted such that the average $b = b_{\sigma_L}$, which dominates the integral on the right-hand side of Eq. (14), is related to Q^2 just via the equality $b_{\sigma_L}^2 = \lambda/Q^2$. In other words, for the longitudinal structure function, the virtuality that corresponds to the dominant transverse distance b_{σ_L} is just the virtuality of the process. This yields $\lambda \sim 8.5$ for $x = 10^{-3}$.

In the same fashion, we can now rewrite the amplitude for diffractive vector meson production as

$$\begin{aligned} \mathcal{A}_{\gamma_L^*N \rightarrow VN} &\propto \alpha_s(Q_{\text{eff}}^2) x G_N(x, Q_{\text{eff}}^2) \\ &\times \int d z d^2 b \phi_{\gamma_L^*}(z, b) b^2 \phi_V(z, b), \end{aligned} \quad (16)$$

where we pulled the gluon density at an average $b = b_V$ out of the integral, i.e., $Q_{\text{eff}}^2 \sim \lambda/b_V^2$, and with the $q\bar{q}$ leading Fock state light-cone wave function of the vector meson $\phi_V(z, b)$. In Fig. 2, we show b_V and Q_{eff}^2 for the longitudinal structure function as well as for diffractive production of (longitudinally polarized) ρ^0 , J/ψ , and Υ mesons. The wave functions $\phi_V(z, b)$ that were used to evaluate Eq. (16) will be discussed in more detail later.

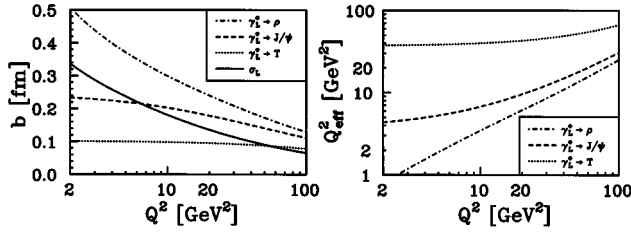


FIG. 2. Average transverse distances effective in the evaluation of the longitudinal structure function as well as for diffractive production of longitudinally polarized ρ° , J/ψ , and Y mesons. Also shown are the resulting effective scales Q_{eff}^2 for diffractive vector meson production.

It can be seen from Fig. 2 that the relevant transverse distances for ρ° electroproduction are larger than those characteristic for the longitudinal structure function, i.e., $b_\rho(Q^2) > b_{\sigma_L}(Q^2)$. Therefore, for ρ° production, the virtuality Q_{eff}^2 that enters in the argument of $\alpha_s(x, Q_{\text{eff}}^2) x G_N(x, Q_{\text{eff}}^2)$ is smaller than Q^2 . We find, to leading order,

$$b_V(Q^2) \approx b_{\sigma_L}(Q_{\text{eff}}^2), \quad (17)$$

which, for ρ° production, yields $Q_{\text{eff}}^2 \approx Q^2 [b_{\sigma_L}(Q^2)/b_V(Q^2)]^2$. Our Eq. (17) is an approximate relation designed to overcome the scale ambiguity which is inherent to leading order calculations. This ‘‘rescaling of hard processes’’ effectively relates the scales in different processes via the dominant $q\bar{q}$ distances in the respective quark loops. We termed this ‘‘ Q^2 rescaling’’ in Ref. [4]. The difference between Q_{eff}^2 and Q^2 indicates that substantial next-to-leading order corrections should be present in those processes. Applying the same method to J/ψ and Y production yields a Q_{eff}^2 which is significantly larger than the estimate $\bar{Q}^2 = (Q^2 + M_V^2)/4$ of Refs. [15,16]. Figure 2 also indicates that the relevant transverse distances are small, and hence the QCD factorization theorem is applicable, for ρ° production at large Q^2 and heavy meson photo- and electroproduction.

D. Production of transversely polarized vector mesons

The discussion in the above refers to the production of longitudinally polarized vector mesons only. For light vector mesons, the formalism at hand cannot be extended to transverse polarizations because of the endpoint singularities, i.e., the contribution from very asymmetric $q\bar{q}$ pairs with $z \sim 0$ or 1, where nonperturbative effects dominate. For the production of heavy quarkonia $Q\bar{Q}$, when $\alpha_s(M_Q^2) \ll 1$ and $q_0/4M_Q^2 \gg r_T$, however, effects of large transverse distances are strongly suppressed. Here, r_T is the radius of the hadron target. So, the production of transversely polarized heavy quarkonia can be legitimately evaluated using the QCD factorization theorem. At the same time, for $Q^2 \gg M_V^2$ the endpoint contribution ($z \sim 0$ or 1) is enhanced in the amplitude for the diffractive electroproduction of transversely polarized vector mesons. Thus, the region of applicability of nonrelativistic wave function models for heavy quarkonia to the production of transversely polarized vector mesons (but not

of the applicability of the QCD factorization theorem) is restricted by the kinematical constraint $Q^2 \leq M_V^2$.

Employing the notations of Ref. [2], the wave functions of longitudinally and transversely polarized photons and heavy vector mesons can be expressed as

$$\phi_{\gamma_L}^{\lambda_1\lambda_2} = 2Qz(1-z)\phi_\gamma(z,b)\delta_{-\lambda_2}^{\lambda_1}, \quad (18)$$

$$\begin{aligned} \phi_{\gamma_T}^{\lambda_1\lambda_2} = & m \begin{pmatrix} \mp 1 \\ -i \end{pmatrix} \phi_\gamma(z,b)\delta_{\lambda_2}^{\lambda_1} \\ & + \begin{pmatrix} i(2z-1)\hat{b}_x \mp \hat{b}_y \\ \pm \hat{b}_x + i(2z-1)\hat{b}_y \end{pmatrix} \frac{\partial \phi_\gamma(z,b)}{\partial b} \delta_{-\lambda_2}^{\lambda_1}, \end{aligned} \quad (19)$$

$$\phi_{V_L}^{\lambda_1\lambda_2} = -2M_V\phi_V(z,b)\delta_{-\lambda_2}^{\lambda_1}, \quad (20)$$

$$\phi_{V_T}^{\lambda_1\lambda_2} = \frac{m}{z(1-z)} \begin{pmatrix} \mp 1 \\ -i \end{pmatrix} \phi_V(z,b)\delta_{\lambda_2}^{\lambda_1}, \quad (21)$$

where

$$\phi_\gamma(z,b) = K_0(b\sqrt{Q^2z(1-z)+m^2}), \quad (22)$$

and $\phi_V(z,b)$ refer to the $q\bar{q}$ light-cone wave functions of the photon and the heavy vector meson, respectively. For the derivation of Eqs. (20) and (21) it was assumed, in line with the nonrelativistic character of heavy quarkonium, that, in the center of mass system, the vector meson’s wave function is a pure angular momentum $L=0$ state. This selects spin $S=0$ (or helicities $\lambda_2 = -\lambda_1$) for the longitudinal polarization and $S=1$ (or $\lambda_2 = \lambda_1$) for the transverse polarizations, with the same spatial wave function $\phi_V(z,b)$. Here, $\lambda_{1,2}$ are the helicities of the quark and antiquark, respectively. For transverse polarization, the restriction through the wave function of heavy quarkonia selects the component in the wave function of the virtual photon which is proportional to the mass of the heavy quark. This is just opposite to the production of mesons built of light quarks where this component in the photon’s wave function is negligible [27].

This gives for the kernels of the longitudinal and transverse amplitudes:

$$\begin{aligned} V_L(z,b) &= \frac{1}{2} \sum_{\lambda_1\lambda_2} \phi_{\gamma_L}^{\lambda_1\lambda_2\dagger} \phi_{V_L}^{\lambda_1\lambda_2} \\ &= -4QM_V z(1-z)\phi_\gamma(z,b)\phi_V(z,b), \end{aligned} \quad (23)$$

$$V_T(z,b) = \frac{1}{4} \sum_{\lambda_1\lambda_2} \phi_{\gamma_T}^{\lambda_1\lambda_2\dagger} \phi_{V_T}^{\lambda_1\lambda_2} = \frac{m^2}{z(1-z)} \phi_\gamma(z,b)\phi_V(z,b). \quad (24)$$

Note that in the limit $z \approx \frac{1}{2}$ and $M_V \approx 2m$, Eqs. (23) and (24) yield the naive prediction $\sigma_L/\sigma_T = (V_L/V_T)^2 \approx Q^2/M_V^2$ for the production ratios of longitudinal to transverse polarizations. Also, because of the nonrelativistic ansatz for the vector meson’s wave function, the spin structure of Eq. (24) is such that there is no azimuthal asymmetry. This is qualitatively different from diffractive two-jet production in deep inelastic scattering [28]. Note, however, that in a fully relativistic description such an azimuthal asymmetry would ap-

pear also for diffractive production of transversely polarized vector mesons due to the admixture of a $L=2, S=1$ component (to the standard $L=0, S=1$ state). Note, also, that the nonrelativistic approximation to the light-cone wave function of transversely polarized heavy quarkonia becomes questionable for the diffractive electroproduction in the limit $Q^2 \gg M_V^2$. This is because, in this kinematics, the end point contributions $z=0$ and $z=1$ are enhanced. But in QCD, in variance from nonrelativistic quarkonium models, the wave function at asymptotical Q^2 should be such that $V_T \propto z(1-z)$. Such a behavior follows from the analysis of PQCD diagrams for the wave function of heavy quarkonia. This complication is practically unimportant because, in this kinematics, the production of longitudinally polarized heavy quarkonia dominates.

Putting everything together, the factor $T(Q^2)$, which accounts for effects related to the quark motion in the produced vector meson, and the correction factor $R(Q^2)$, which parametrizes the relative contribution of the transverse production, can be written in transverse impact parameter space as

$$T(Q^2) = \left[\frac{(Q^2 + 4m^2)^2}{4} \times \frac{\int dz z(1-z) \int db \phi_V(z, b) b^3 \phi_\gamma(z, b)}{\int [dz/z(1-z)] \phi_V(z, b=0)} \right]^2, \quad (25)$$

This shows that, for these processes, a decomposition over twists is really an expansion in powers of b^2 , and ‘‘leading twist’’ is equivalent to the $b \rightarrow 0$ limit, i.e., to considering very small transverse distances (or ‘‘pointlike hadrons’’) only. Specific to heavy quarkonium production is that, in addition to neglecting k_t^2/Q^2 and m^2/Q^2 terms as for light quarks, one also neglects terms of the form k_t^2/m^2 .

Note that the expressions (27) and (28) are stringent QCD predictions for heavy quark production deduced in an expansion where m is considered as a large parameter. The leading term is proportional to the mass of the heavy quark in difference from light quark production where the leading term is proportional to the quark’s transverse momentum. So, the formulas deduced in this paper cannot be smoothly interpolated to the limit of the zero quark mass.

Furthermore, in the static limit of $m \rightarrow \infty$, which implies $\phi_V(z, k_t) = \delta(z - \frac{1}{2}) \phi_V(k_t)$ and $M_V = 2m$, the correction factors $T(Q^2)$, $R(Q^2)$, $T_{LT}(Q^2)$, and $R_{LT}(Q^2)$ reduce to

$$T(Q^2) \rightarrow 1 - 32 \frac{\langle k_t^2 \rangle}{Q^2 + 4m^2}, \quad (29)$$

$$R(Q^2) \rightarrow 1, \quad (30)$$

$$R(Q^2) = \left[\frac{m^2}{4M_V^2} \frac{\int [dz/z(1-z)] \int db \phi_V(z, b) b^3 \phi_\gamma(z, b)}{\int dz z(1-z) \int db \phi_V(z, b) b^3 \phi_\gamma(z, b)} \right]^2, \quad (26)$$

where we used again $\phi_\gamma(z, b)$ of Eq. (22). The $T(Q^2)$ and $R(Q^2)$, displayed in the above, are the leading expressions to order $1/(Q^2 + 4m^2)$, and they constitute our main original new results. They are related to the quantities given in Eqs. (7) and (8) simply via a two-dimensional Fourier transformation.

E. Leading twist expressions and comparison with other k_t -suppression estimates

Note that the suppression factor $T(Q^2)$ of Eq. (25) and the transverse to longitudinal production ratio $R(Q^2)$ of Eq. (26) have contributions from leading and nonleading twist. The corresponding leading twist expressions can be deduced by pulling the vector meson’s wave function $\phi_V(z, b)$ at $b=0$ out of the integral, i.e., by replacing $\phi_V(z, b)$ with $\phi_V(z, 0)$. The latter is equivalent to setting in the photon’s wave function, $\phi_\gamma(z, k_t)$ of Eq. (5), k_t to zero after differentiation, and it yields

$$T_{LT}(Q^2) = \left[\frac{\int [dz/z(1-z)] \{ [Q^2 + 4m^2] / \{ Q^2 + [m^2/z(1-z)] \} \}^2 \phi_V(z, b=0)}{\int [dz/z(1-z)] \phi_V(z, b=0)} \right]^2, \quad (27)$$

$$R_{LT}(Q^2) = \left[\frac{m^2}{4M_V^2} \frac{\int [dz/z^3(1-z)^3] \{ 1 / [[Q^2 + m^2] / z(1-z)] \}^2 \phi_V(z, b=0)}{\int [dz/z(1-z)] \{ 1 / [[Q^2 + m^2] / z(1-z)] \}^2 \phi_V(z, b=0)} \right]^2. \quad (28)$$

$$T_{LT}(Q^2) \rightarrow 1, \quad (31)$$

$$R_{LT}(Q^2) \rightarrow 1, \quad (32)$$

where

$$\langle k_t^2 \rangle \equiv \frac{\int d^2 k_t k_t^2 \phi_V(k_t)}{\int d^2 k_t \phi_V(k_t)}. \quad (33)$$

Recently, in two investigations [16,26], effects of the transverse quark motion on diffractive charmonium production were discussed. In Ref. [26], the presence of a Q^2 independent correction was claimed, which contradicts the strict asymptotic QCD result of [2]. For photoproduction, the correction term of Ref. [26] is by a factor of 24 smaller than our leading twist, order $\mathcal{O}(k_t^2)$ correction of Eq. (29). To be able to compare with the result of Ref. [16], we use the expression of $T(Q^2)$ in transverse momentum space, i.e., Eq. (7). The correction factor for J/ψ photoproduction discussed in Ref. [16] can be obtained from our $T(Q^2=0)$ of Eq. (7) by

approximating $\Delta_t \phi_\gamma(z, k_t)$ with the respective leading order expression in $\mathcal{O}(k_t^2/m^2)$ and by neglecting the longitudinal relative motion of the quarks, i.e., by setting $\phi_V(z, k_t) = \delta(z - 1/2) \phi_V(k_t)$. In addition, a Gaussian form for the wave function $\phi_V(k_t)$ was assumed in Ref. [16]. All of these approximations diminish the relative contribution of large quark momenta, and hence result in a significantly weaker suppression. This was already pointed out in Ref. [4] in a footnote.

F. The t slope of diffractive vector meson production

It was demonstrated in Ref. [2] that, in the limits of fixed small x and $Q^2 \rightarrow \infty$, the t slope of the vector meson electroproduction cross section should be flavor independent and determined solely by the slope of the gluon-nucleon scattering amplitude. However, the Q^2 dependence of the average quark separation— $\langle b(Q^2) \rangle_{Q^2 \rightarrow \infty} \rightarrow 0$ in the production amplitude of Eq. (16) presented in Fig. 2—leads to a Q^2 and flavor dependence of the t slope. This effect can easily be incorporated into Eq. (16) by evaluating the matrix element of the factor $e^{-iz\vec{q}_t \cdot \vec{b}} + e^{iz\vec{q}_t \cdot \vec{b}} - e^{-i(z\vec{q}_t + \vec{l}) \cdot \vec{b}} - e^{i(z\vec{q}_t + \vec{l}) \cdot \vec{b}}$ between the wave functions of the photon and the vector meson. Here, \vec{l} is transverse momentum of one of the exchanged gluons, \vec{q}_t is the transverse component of the four-momentum transferred to the target nucleon and $t = -|\vec{q}_t|^2$ (we neglect here terms proportional to x). This amplitude can be written, in factorized form, as a convolution integral over l_t of the hard blob and the nondiagonal gluon distribution in the target at a virtuality l^2 . Since b is small, it is reasonable to decompose this expression over powers of b up to b^2 . After that, the respective amplitude factorizes into a product of the hard blob (accounting for the t dependence) and the nondiagonal gluon distribution in the target at virtuality $\sim \lambda/b^2$. Note that since the momentum integrals in the hard blob depend on b^2 only logarithmically, the b -dependent term in the slope of the gluon-nucleon amplitude should decrease with b at least as $b^2/\ln(b/b_0)$. So we can neglect it, to a first approximation, as compared to the effects of the form factor in the $\gamma_L^* \rightarrow V$ vertex, which are proportional to b^2 . Besides, studies of soft elastic scattering indicate that even for such processes the main contribution to the t dependence of the amplitude comes from hadron form factors (if the energy is not so large that Gribov diffusion contributes). Hence, we expect that, in the hard regime, the b -dependent term in the amplitude will have a numerically small coefficient, in addition to being suppressed by the $\ln(b/b_0)$ factor.

Thus, effectively, one should include, similar as for a form factor of a $Q\bar{Q}$ bound state [29], in the integral on the right-hand side of Eq. (16) an additional factor of $e^{-iz\vec{q}_t \cdot \vec{b}}$, where \vec{q}_t is the three-momentum transferred to the target nucleon and $t = -|\vec{q}_t|^2$. Parametrizing as usual $d\sigma/dt = A e^{B_V t}$ for small t , we can calculate the Q^2 dependence of $\Delta B_V(Q^2) \equiv B_V(Q^2) - B_V(Q^2 \rightarrow \infty)$, i.e., the contribution of the hard blob of Fig. 1 to the t dependence of the cross section, from

$$\Delta B_V(Q^2) = \frac{1}{2} \frac{\int dz d^2b \phi_{\gamma_L^*}(z, b) \sigma_{q\bar{q}N}(x, b) \phi_V(z, b) z^2 b^2}{\int dz d^2b \phi_{\gamma_L^*}(z, b) \sigma_{q\bar{q}N}(x, b) \phi_V(z, b)}, \quad (34)$$

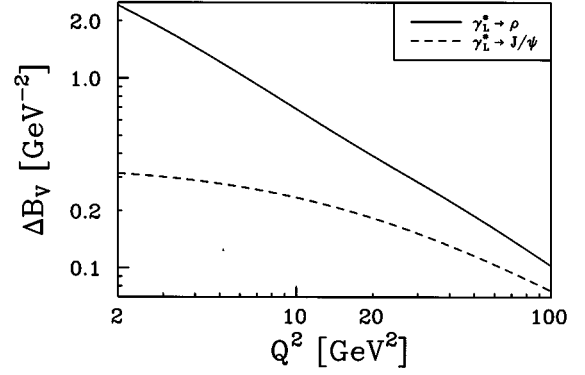


FIG. 3. The contribution of the hard blob to the t slope of diffractive electroproduction of longitudinally polarized ρ^0 and J/ψ vector mesons.

with the color dipole cross section $\sigma_{q\bar{q}N}(x, b)$ of Eq. (10), and $\phi_{\gamma_L^*}(z, b)$ of Eq. (15) and $\phi_V(z, b)$, the $q\bar{q}$ light-cone wave functions of the photon and the vector meson, respectively. Results of such a calculation are presented in Fig. 3 for J/ψ and ρ -meson production. Thus, the dependence of the cross section on t contains information on the distribution of color in the produced vector mesons. Note that the experimentally observed t slope for J/ψ photoproduction and electroproduction and ρ^0 electroproduction at large Q^2 is of the order of $B_V \approx 4 - 5 \text{ GeV}^{-2}$. The main conclusion from Fig. 3 is thus that the t slope of diffractive vector meson production is determined mostly by the gluon-nucleon scattering amplitude, the differences in B_V between different flavors are small for realistic Q^2 , and they vanish in the $Q^2 \rightarrow \infty$ limit.

We have demonstrated in Ref. [4] that, at sufficiently small x , i.e., close enough to the low x range probed at HERA, higher twist effects may become important. This would also lead to a breakdown of the universality of the t slope. This effect can be estimated by including double scatterings of the $q\bar{q}$ pair off the nucleon [30,4,31]. Neglecting the small difference of the average b for single and double scattering, we can calculate the t slope of the rescattering amplitude from

$$\left. \frac{d\sigma}{dt} \right|_{\text{screen}} = \left. \frac{d\sigma}{dt} \right|_{t=0} \cdot \left| e^{Bt/2} - \frac{1}{16\pi B} \frac{\langle \sigma_{q\bar{q}N}^2(x, b) \rangle}{\langle \sigma_{q\bar{q}N}(x, b) \rangle} \right. \\ \left. \times (e^{Bt/4} + r e^{\tilde{B}t/4}) \right|^2. \quad (35)$$

Here $d\sigma/dt|_{t=0}$ is the cross section given in Eq. (3) and

$$\frac{\langle \sigma_{q\bar{q}N}^2(x, b) \rangle}{\langle \sigma_{q\bar{q}N}(x, b) \rangle} = \frac{\int dz d^2b \phi_{\gamma_L^*}(z, b) \sigma_{q\bar{q}N}^2(x, b) \phi_V(z, b)}{\int dz d^2b \phi_{\gamma_L^*}(z, b) \sigma_{q\bar{q}N}(x, b) \phi_V(z, b)}, \quad (36)$$

where $\sigma_{q\bar{q}N}(x, b)$ is again the color dipole cross section of Eq. (10). The quantity denoted r is the ratio of the inelastic to elastic diffractive production of vector mesons at large Q^2 , and experimentally $r \approx 0.2$. \tilde{B} is the slope of the inelastic production, i.e., the $\gamma_L^* + p \rightarrow V + X$ process, and it is, so far,

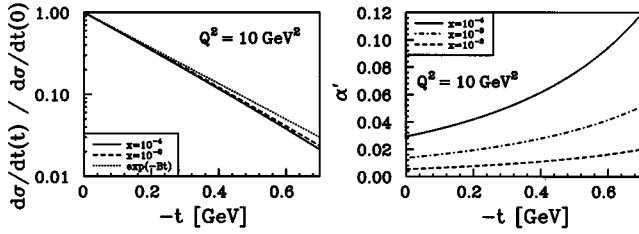


FIG. 4. The t dependence of the diffractive vector meson production cross section, i.e., $d\sigma/dt|_{\text{screen}}/d\sigma/dt|_{t=0}$ of Eq. (35), and the change of the t slope with energy, i.e., $\alpha'(t)$ of Eq. (37). Results are shown for ρ^0 electroproduction at $Q^2=10 \text{ GeV}^2$.

not well known experimentally. Since for this process, in difference from the elastic production, there is essentially no form factor at the nucleon vertex, the quantity \bar{B} is much smaller than the elastic slope B , and a natural guess is $\bar{B} \approx 1-2 \text{ GeV}^{-2}$. Experimentally [18], the ratio of inelastic to elastic J/Ψ production is of the order of 0.5–0.7, i.e., $rB/\bar{B} \sim 0.5-0.7$.

For our numerical estimates we set $r=0.25$, $B(x \sim 10^{-2})=5 \text{ GeV}^{-2}$, and $\bar{B}=2 \text{ GeV}^{-2}$. In Fig. 4(a) we show the t dependence of the diffractive ρ^0 electroproduction cross section, i.e., $d\sigma/dt|_{\text{screen}}/d\sigma/dt|_{t=0}$ of Eq. (35). Since the color dipole cross section $\sigma_{q\bar{q}N}(x,b)$ of Eq. (10) is proportional to $xG_N(x,\lambda/b^2) \propto x^{0.2-0.3}$, Eq. (35) leads to an increase of the t slope with decreasing x . This can be seen from Fig. 4(a), where we compare $d\sigma/dt|_{\text{screen}}$ for $x=10^{-2}$ (dashed line) and $x=10^{-4}$ (solid line) with the leading twist result e^{-Bt} (dotted line).

The change of the t -slope with “energy” $s = Q^2/x$ is usually parameterized in the form

$$B(s) = B(s_0) + 2\alpha'(t) \ln \left[\frac{s}{s_0} \right], \quad (37)$$

and the quantity α' increases with $-t$. This can be seen from Fig. 4(b), where we show $\alpha'(t)$ as a function of t for various x . Again, due to the increase of the color dipole cross section $\sigma_{q\bar{q}N}(x,b)$ with energy, the increase of α' with $-t$ is more dramatic for smaller x (larger energies). Note that the numerical results shown in Fig. 4 refer to ρ^0 electroproduction at $Q^2=10 \text{ GeV}^2$. As can be seen from Fig. 2, the respective Q_{eff}^2 is very similar to the Q_{eff}^2 relevant for J/ψ photoproduction, and hence the numerical estimates shown in Fig. 4 should thus be approximately valid also for J/ψ photoproduction. Figure 4 suggests that a study of the t slopes of diffractive vector meson production may yet provide another sensitive probe of the dynamics of hard diffraction.

III. THE QUARKONIUM LIGHT-CONE WAVE FUNCTION

In order to be able to evaluate the asymptotic correction η_V of Eq. (2) as well as the $T(Q^2)$ and $R(Q^2)$ of Eqs. (7) and (8) or Eqs. (25) and (26), we need the light-cone wave function of the $q\bar{q}$ leading Fock state in the vector meson. We will discuss this quantity in detail in this section. Note

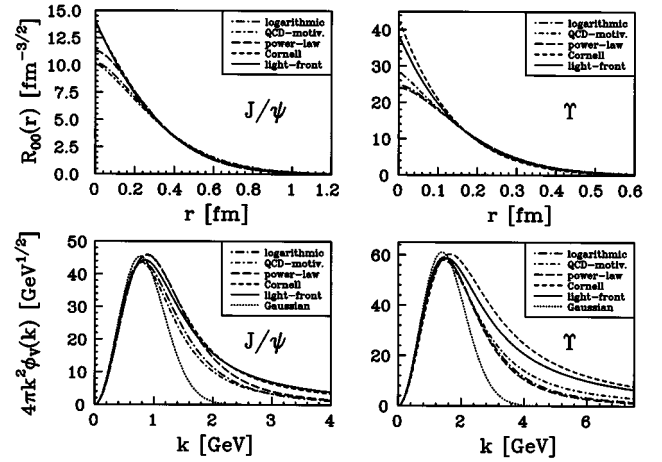


FIG. 5. The nonrelativistic quarkonium wave functions for the heavy ground state mesons J/ψ and Y from various potential models [5–8] and a light-front QCD bound state calculation [9]. In the lower part of the figure, we also show a Gaussian fit adjusted to reproduce $\phi_V(k)$ at small k (dotted lines).

also that, as a result of the factorization theorem in QCD, it is the distribution of bare (current) quarks that enter in the description of these hard processes, and therefore, *a priori* there should be no simple relation between this quantity and nonrelativistic potential models.

A. Nonrelativistic potential models

Due to the large value of the quark mass, it is generally assumed that a nonrelativistic ansatz with a Schrödinger equation and an effective confining potential yields a fairly good description of heavy quarkonium bound states. The various models—see Ref. [32] for an overview—differ in the functional form of the potential, but they all give a reasonable account of the $c\bar{c}$ and $b\bar{b}$ bound state spectra and decay widths. The same holds for the light-front QCD bound state calculation of Ref. [9]. In Fig. 5, we display the quantities $R_{00}(r)$ [normalized such that $\int dr r^2 |R_{00}(r)|^2 = 1$] and $4\pi^2 k^2 \phi_V(k)$ (normalized such that $[1/(2\pi)^3] \times \int d^3k |\phi_V(k)|^2 = 1$). For the latter, we also plot a Gaussian fit adjusted to reproduce $\phi_V(k)$ at small k . It turns out that the wave functions can be well approximated at small k by Gaussian fits, while, at large k , they fall off much slower and they display a significant high momentum tail.

Note that for our actual numerical calculations we will restrict our considerations to the models of Refs. [5], [6], and [9] for which the mass of the constituent quark is close to the mass of the bare current quark, i.e., $m_c \approx 1.5 \text{ GeV}$ and $m_b \approx 5.0 \text{ GeV}$. This is necessary to keep a minimal correspondence with the QCD formulas for hard processes which are expressed through the distribution of bare quarks [2].

In Fig. 6, we show the contributions of the different regions in momentum space to the integral $\int d^3k \phi_V(k)$ for the potential model of Ref. [5] (logarithmic potential). This integral appears, for instance, in the expression for the $V \rightarrow e^+ e^-$ decay width. Especially for J/ψ mesons, the conventional nonrelativistic potential models lead to a significant high momentum tail in the respective wave functions,

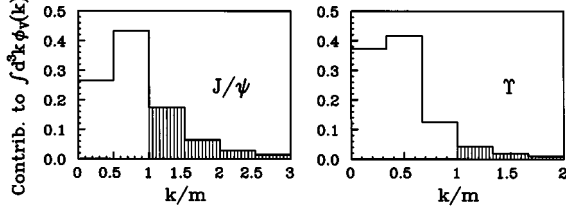


FIG. 6. Histogram of the relative contributions of the different regions in momentum space to the integral $\int d^3k \phi_V(k)$ for the potential model of Ref. [5].

and the contribution of the relativistic region² $v/c \geq 1$ (or $k \geq m$) to the integral $\int d^3k \phi_V(k)$ (the shaded area in Fig. 6) becomes large. For the potential model of Ref. [5], the contribution of the relativistic region $k \geq m$ to the integral under consideration is 30% for J/ψ (and $\leq 10\%$ for Υ). Also, for the J/ψ , half of the integral comes from the region $k \geq 0.7m$. This is in line with the QCD prediction of large relativistic corrections to the $c\bar{c}$ bound state equations [10], and it puts the feasibility of a nonrelativistic description of heavy quarkonium production in high energy processes seriously into question.

The fact that, in particular for the J/ψ meson, our numerical analysis yields a significant value for the high momentum component in the respective nonrelativistic wave functions is a very important result which should have consequences far beyond the topic of diffractive vector meson production. The large high momentum tail, visible in the lower part of Fig. 5, and the significant contribution of the relativistic region to the integral $\int d^3k \phi_V(k)$, displayed in Fig. 6, indicate that the J/ψ meson is not really a nonrelativistic system. This puts the nonrelativistic ansatz employed in the various potential models [5–8] as well as in the light-front QCD bound state calculation [9] seriously into question.

However, there are more inconsistencies between the nonrelativistic ansatz and the hard reaction considered here. For once, the requirement of self-consistency dictates that since in our formulae we use the gluon distribution $xG_N(x, Q^2)$ extracted from the data within a certain renormalization scheme ($\overline{\text{MS}}$), we are indebted to use the bare quark mass defined within the same scheme. This means that, in our final formulas in Eqs. (6)–(8), (25)–(28), the pole or constituent quark mass m has to be replaced by the running mass $m_{\text{run}}(Q_{\text{eff}}^2)$, where [33]

$$m^2 \rightarrow m_{\text{run}}^2(Q_{\text{eff}}^2) = m^2 \left(1 - \frac{8\alpha_s}{3\pi} \right). \quad (38)$$

Here, α_s is evaluated at Q_{eff}^2 , i.e., at the effective scale of the reaction determined via the so-called “rescaling of hard processes.” This is another consequence of the difference between soft, nonperturbative physics (as described, for instance, by nonrelativistic quarkonium potential models) and hard perturbative QCD, and it further stresses the inadequa-

²Evidently, relativistic effects should become important already at significantly smaller k .

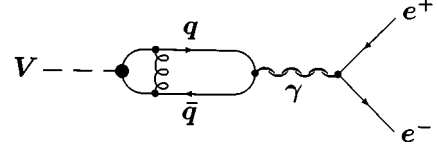


FIG. 7. The QCD radiative correction [12] to the $V \rightarrow e^+e^-$ decay width.

ties of a naive straightforward application of nonrelativistic potential models in this context.

Another mismatch between the soft nonrelativistic and the hard light-cone approach appears within the evaluation of the $V \rightarrow e^+e^-$ decay width. When $\Gamma_{V \rightarrow e^+e^-}$ is calculated from the nonrelativistic wave function $\phi_V(k)$ via

$$\Gamma_{V \rightarrow e^+e^-} = \frac{16\pi\alpha^2 e_q^2}{M_V^2} \left(1 - \frac{16\alpha_s}{3\pi} \right) \left| \int \frac{d^3k}{(2\pi)^3} \phi_V(k) \right|^2, \quad (39)$$

a QCD correction factor [12] appears, $1 - 16\alpha_s/3\pi$, which can be numerically large ($16\alpha_s/3\pi \approx 0.35 - 0.65$ for J/ψ), while no such term is present within the relation [2] with the light-cone $q\bar{q}$ wave function $\phi_V(z, k_t)$,

$$\Gamma_{V \rightarrow e^+e^-} = \frac{32\pi\alpha^2 e_q^2}{M_V} \left| \int dz \int \frac{d^2k_t}{16\pi^3} \phi_V(z, k_t) \right|^2. \quad (40)$$

The appearance of this correction factor is the main differences between the various nonrelativistic potential models and a “true” QCD approach, in which the light-cone wave function of the minimal $q\bar{q}$ Fock component in the vector meson is employed. It is a radiative correction to the matrix element of the electromagnetic current calculated, essentially, while neglecting quark Fermi motion effects. The respective Feynman diagram is shown in Fig. 7.

The correction arises from the exchange of a gluon between the quark and the antiquark in the vector meson with fairly large transverse momentum, $\langle l_t \rangle \approx m$. The physical interpretation of the $1 - 16\alpha_s/3\pi$ correction factor is that it “undresses” the constituent quarks, which are the relevant degrees of freedom of the nonrelativistic wave function, back to current quarks, which, in turn, are the degrees of freedom the light-cone wave function refers to and to which the $V \rightarrow e^+e^-$ decay width is ultimately connected. This, once more, underlines the limits of applicability of nonrelativistic potential models in that context. Note that this radiative correction is also present in the light-front QCD bound state calculation of Ref. [9] because also there the relevant degrees of freedom are dressed constituent and not bare current quarks.

B. The light-cone wave function

Leaving these issues behind for the moment, we can, in principle, deduce a light-cone wave function $\phi_V(z, k_t)$ appropriate for the evaluation of time-ordered perturbation theory diagrams from the nonrelativistic wave function $\phi_V(k)$. This requires a translation of conventional nonrelativistic diagrams into light-cone perturbation theory diagrams. This, in turn, can be achieved by the purely kinematical identification

of the Sudakov variable z , which denotes the fraction of the plus component of the meson's momentum carried by one of the quarks, with

$$z = \frac{1}{2} \left(1 + \frac{k_z}{\sqrt{k^2 + m^2}} \right). \quad (41)$$

This yields

$$k^2 \rightarrow \frac{k_t^2 + (2z-1)^2 m^2}{4z(1-z)}, \quad (42)$$

$$d^3k \rightarrow \frac{\sqrt{k_t^2 + m^2}}{4[z(1-z)]^{3/2}} dz d^2k_t, \quad (43)$$

where $\pm \vec{k}_t$ are the quarks' transverse momenta. This, together with the conservation of the overall normalization of the wave function,

$$1 = \int \frac{d^3k}{(2\pi)^3} |\phi_V(k)|^2 = \int dz \int \frac{d^2k_t}{16\pi^3} |\phi_V(z, k_t)|^2 \quad (44)$$

then gives a relationship between the light-cone and the nonrelativistic wave function:

$$\phi_V(z, k_t) = \sqrt[4]{\frac{k_t^2 + m^2}{4[z(1-z)]^3}} \phi_V \left(k = \sqrt{\frac{k_t^2 + (2z-1)^2 m^2}{4z(1-z)}} \right). \quad (45)$$

From $\phi_V(z, k_t)$ we then calculate the quarkonium's wave function in transverse impact parameter space $\phi_V(z, b)$ through a two-dimensional Fourier transformation,

$$\phi_V(z, b) = \int \frac{d^2k_t}{16\pi^3} e^{i\vec{k}_t \cdot \vec{b}} \phi_V(z, k_t). \quad (46)$$

Obviously, the nonrelativistic quarkonium model, designed as a description of the $q\bar{q}$ constituent quark component—including the $1 - 16\alpha_s/3\pi$ factor which accounts for radiative corrections—does not include gluon emission at a higher resolution. So it is not surprising that the $\phi_V(z, b)$ that we find does not display the expected asymptotic behavior [11]:

$$\phi_V(z, b=0) \neq z(1-z). \quad (47)$$

This is illustrated in Fig. 8. There, we compare the quarkonium wave functions $\phi_V(z, b=0)$ obtained in that manner from the nonrelativistic potential models of Refs. [5], [6], and [9] with a hard wave function $\phi_V^{\text{hard}}(z, b=0) = a_0 z(1-z)$, where the parameter a_0 was adjusted by means of Eq. (40) to reproduce the vector meson's leptonic decay width $\Gamma_{V \rightarrow e^+ e^-}$. For transversely polarized vector mesons, the light-cone wave function should behave as $\propto z^2(1-z)^2$. This follows from the analysis of respective PQCD diagrams.

C. Hard physics

We argued in Sec. III A that, although the average properties of heavy quarkonium bound states might, in general, be quite well described within a nonrelativistic framework

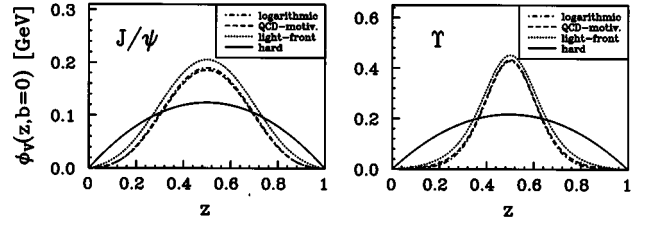


FIG. 8. The quarkonium wave functions $\phi_{J/\psi}(z, b)$ and $\phi_T(z, b)$, for $b=0$. The dot-dashed, dashed, and dotted lines correspond to the nonrelativistic potential models of Refs. [5], [6], and [9], respectively, and the solid lines refer to the ‘‘hard physics’’ limit $\phi_V(z, b=0) \propto z(1-z)$.

due to the large value of the quark mass, there appear significant high momentum (or ‘‘hard physics’’) corrections if observables are considered which crucially depend on short distances.

One example is the leptonic decay width, $\Gamma_{V \rightarrow e^+ e^-}$, which acquires large radiative corrections in a nonrelativistic potential model. An analysis of the respective Feynman diagram, shown in Fig. 7, yields that these corrections arise from relativistic momenta $k \gtrsim m$. Even putting those corrections aside, already the quantity which is related to the decay width in zeroth order, $\int d^3k \phi_V(k)$, contains large contributions from the relativistic region $k \gtrsim m$ (30% for J/ψ for a typical potential model). And when we (purely kinematically) translate the nonrelativistic wave functions into light-cone coordinates, we find that they do not display the expected asymptotic short distance behavior $\phi_V(z, b=0) \propto z(1-z)$ as dictated by perturbative one-gluon exchange.

This suggests that the nonrelativistic potential model wave functions might describe the $q\bar{q}$ leading Fock state in heavy quarkonia for fairly large (average) distances, but the description breaks down in the limit of small distances or high momenta. As these play a crucial role for the processes we are interested in, we designed the following strategy.

First, we extract a light-cone wave function from a nonrelativistic potential model through the purely kinematical transformations of Eqs. (41)–(45), which we then Fourier transform into transverse impact parameter space via Eq. (46). However, we have confidence in that wave function, which we denote $\phi_V^{\text{NR}}(z, b)$, only for transverse distances $b \gtrsim 1/m$, and we expect it to be modified at shorter distances by means of the ‘‘hard physics’’ corrections discussed in the above. We thus set

$$\phi_V(z, b) = \begin{cases} \phi_V^{\text{NR}}(z, b) & \text{for } b \gtrsim b_0, \\ \phi_V^{\text{LC}}(z, b) & \text{for } b < b_0, \end{cases} \quad (48)$$

where $b_0 \sim 1/m$.

The wave function $\phi_V^{\text{LC}}(z, b)$ is then constructed such that (1) $\phi_V(z, b)$ and $\partial \phi_V(z, b)/\partial b$ are continuous at $b = b_0$, (2) $\phi_V^{\text{LC}}(z, b)$ has the correct asymptotic behavior dictated by the perturbative exchange of hard gluons, i.e., $\phi_V^{\text{LC}}(z, b=0) \propto z(1-z)$, and (3) $\phi_V^{\text{LC}}(z, b)$ reproduces the vector meson's leptonic decay width *without* account of the radiative correc-

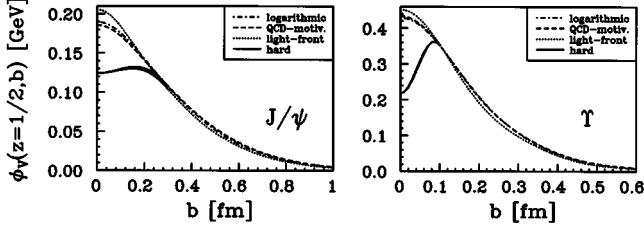


FIG. 9. The quarkonium wave functions $\phi_{J/\psi}(z, b)$ and $\phi_Y(z, b)$, for $z = 1/2$. The dot-dashed, dashed, and dotted lines correspond to the nonrelativistic potential models of Refs. [5], [6], and [9], and the solid lines refer to the inclusion of the ‘‘hard physics’’ corrections of Eqs. (48) and (49) for $b < b_0$. We set $b_0 = 0.3$ fm for J/ψ and $b_0 = 0.1$ fm for Y .

tion term $1 - 16\alpha_s/3\pi$, i.e., Eq. (40) is used to calculate $\Gamma_{V \rightarrow e^+e^-}$. We expand $\phi_V^{LC}(z, b)$ in terms of Gegenbauer polynomials,³

$$\phi_V^{LC}(z, b) = a_0(b)z(1-z) \left(1 + \sum_{n=2,4,\dots} a_n(b)C_n^{3/2}(2z-1) \right), \quad (49)$$

and we assume that the coefficients $a_i(b)$ depend on b^2 only through second order, i.e., $a_i(b) = a_{i0} + a_{i1}b^2 + a_{i2}b^4$. This, together with the conditions (1)–(3) is sufficient to unambiguously determine $\phi_V^{LC}(z, b)$. In our actual numerical calculations, we set $b_0 = 0.3$ fm for J/ψ and $b_0 = 0.1$ fm for Y . Respective wave functions are shown in Fig. 9. The dot-dashed, dashed, and dotted lines show the nonrelativistic wave functions $\phi_V^{NR}(z = 1/2, b)$ before the ‘‘hard physics’’ corrections discussed in this subsection were imposed, and the solid lines depict the modified wave functions $\phi_V^{LC}(z = 1/2, b)$ of Eq. (49).

Note that the ‘‘hard physics’’ corrections, which we introduced in the above, address effects that are of higher order in an expansion in $1/m$. But the prescription of modifying the wave function at $b < b_0$ only accounts for some (but not all) corrections to this order. We thus emphasize that the corrections outlined in this subsection are a model estimate only.

D. Vector meson production

For the potential models of Refs. [5], [6], and [9], the nonrelativistic wave functions $\phi_V^{NR}(z, b)$ yield values for the asymptotic correction factor η_V of Eq. (2) of $\eta_{J/\psi} \approx 2.3$ – 2.4 and $\eta_Y \approx 2.1$ – 2.2 if the ‘‘hard physics’’ correction outlined in the last section is not considered. While, with that correction, they yield $\eta_V = 3$. Note that the static limit, i.e., $\phi_V(z, b) = \delta(z - 1/2)\phi_V(b)$, gives $\eta_V = 2$.

³The expansion in Gegenbauer polynomials has nothing to do with renormalization group methods. They provide a complete basis for the $\phi_V(z, b)$ under consideration and allow a smooth interpolation between the $b \rightarrow 0$ and $b \geq 1/m$ regimes. The series in Eq. (49) is terminated when convergence is achieved, which, in practice, is at $n \sim 10$.

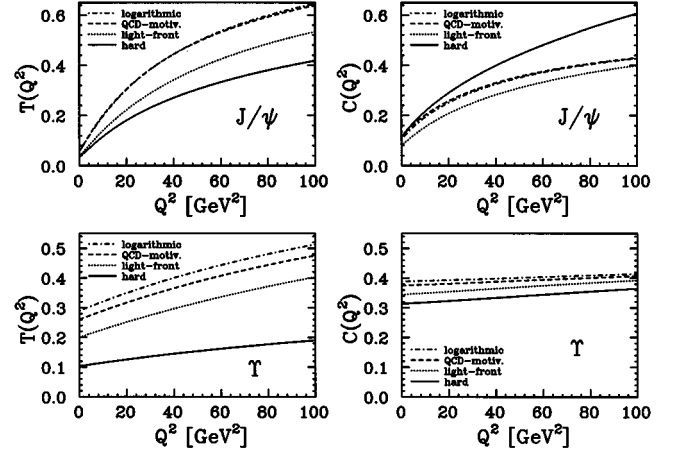


FIG. 10. The Fermi motion suppression factor $T(Q^2)$ of Eq. (7) and the finite Q^2 correction $C(Q^2)$ of Eq. (51), for J/ψ and Y production.

Furthermore, in line with the discussion in Sec. III A, we do not use the pole mass m in our final formulas, but we replace it with the running mass m_{run} , as given by Eq. (38). We can then use the wave functions $\phi_V(z, b)$, that we constructed in the last two subsections, to calculate the correction factors of Eqs. (7) and (8) or Eqs. (25) and (26). Putting everything together, we can rewrite the forward differential cross section for photoproduction and electroproduction of heavy vector mesons of Eq. (6) as the product of an asymptotic expression and a finite Q^2 correction $C(Q^2)$, where

$$\begin{aligned} \frac{d\sigma_{\gamma^{(*)}N \rightarrow VN}}{dt} \Big|_{t=0} &= \frac{12\pi^3 \Gamma_V M_V^3}{\alpha_{EM} (Q^2 + 4m^2)^4} |\alpha_s(Q_{\text{eff}}^2) (1 + i\beta) x G_N(x, Q_{\text{eff}}^2)|^2 \\ &\times \left(1 + \epsilon \frac{Q^2}{M_V^2} \right) C(Q^2), \end{aligned} \quad (50)$$

with

$$C(Q^2) = \left(\frac{\eta_V}{3} \right)^2 \left(\frac{Q^2 + 4m^2}{Q^2 + 4m_{\text{run}}^2} \right)^4 T(Q^2) \frac{R(Q^2) + \epsilon(Q^2/M_V^2)}{1 + \epsilon(Q^2/M_V^2)}. \quad (51)$$

Here, η_V is the leading twist correction of Eq. (2), the factor $T(Q^2)$ of Eq. (7) accounts for effects related to the quark motion in the produced vector meson, ϵ is the (virtual) photon’s polarization, and the factor $R(Q^2)$ of Eq. (8) parametrizes the relative contribution of the transverse polarization. The pole mass m we set to $m = 1.5$ GeV for J/ψ and to $m = 5.0$ GeV for Y production, and m_{run} is the ‘‘running mass’’ of Eq. (38) which, through Q_{eff}^2 , depends on Q^2 and the vector meson’s wave function.

Results for the Fermi motion suppression factor, $T(Q^2)$ of Eq. (7), and the finite Q^2 correction, $C(Q^2)$ of Eq. (51), are shown in Fig. 10 for J/ψ and Y photoproduction and electroproduction. The calculations are based on vector meson wave functions from the models of Refs. [5], [6], and [9].

The solid line, labeled hard, refers to the inclusion of the ‘‘hard physics’’ corrections of Sec. III C. For the evaluation of $\mathcal{C}(Q^2)$, the photon’s polarization ϵ was set to 1.

It can be seen from that figure that, for reasonable Q^2 , the correction factor $\mathcal{C}(Q^2)$, which measures the suppression of the cross section due to the quark motion in the produced vector meson, is significantly smaller than 1. This shows that the asymptotic expression, i.e., Eq. (50) with the finite Q^2 correction $\mathcal{C}(Q^2)$ set to 1, is valid for extremely large Q^2 only. Note that the ‘‘hard physics’’ corrections of Sec. III C lead to a stronger suppression in $T(Q^2)$, but, at least for J/ψ production, to less suppression in the final correction factor $\mathcal{C}(Q^2)$. The reason for this is, firstly, that the ‘‘hard physics’’ correction increases η_V of Eq. (2) from around 2.1–2.4 to 3, and, secondly, that the running mass m_{run} of Eq. (38) is smaller than the pole mass, which also enhances the cross section. In addition, the relative contribution of the transverse polarizations $R(Q^2)$ of Eq. (8) is very close to 1 both for J/ψ and Y production for all experimentally accessible Q^2 if the ‘‘hard physics’’ corrections are left out. However, at least for J/ψ production, after the ‘‘hard physics’’ corrections are considered, $R(Q^2)$ increases significantly with Q^2 . This, together with the changes through η_V and m_{run} lead to the difference between $T(Q^2)$ and $\mathcal{C}(Q^2)$. The cross sections are enhanced also due to the so-called ‘‘rescaling of hard processes,’’ because the virtuality that enters in the gluon density, Q_{eff}^2 of Eq. (17), is larger than the naive estimate of $\bar{Q}^2 = (Q^2 + M_V^2)/4$. This was discussed in detail in Sec. II C.

Note that for photoproduction, i.e., for $Q^2=0$, only the transverse polarizations are present, and the correction $\mathcal{C}(Q^2)$ of Eq. (51) takes on the form

$$\begin{aligned} \mathcal{C}(0) &\propto T(0)R(0) \\ &\propto \left[\frac{\int [dz/z^2(1-z)^2] \int d^2k_t \phi_V(z, k_t) \Delta_t \phi_\gamma(z, k_t)}{\int [dz/z(1-z)] \int d^2k_t \phi_V(z, k_t)} \right]^2. \end{aligned} \quad (52)$$

The presence of the $1/z^2(1-z)^2$ term strongly enhances smearing in the longitudinal motion, i.e., the contribution of asymmetric $q\bar{q}$ pairs with $z \neq 1/2$ is pronounced.

E. The ratio of Y and J/ψ photoproduction

One can furthermore conclude from Fig. 10, together with our master formula in Eqs. (50) and (51), that, after an eventual luminosity upgrade, a significant production of Y mesons is expected at HERA. The cross section ratio of Y to J/ψ photoproduction (at fixed x) is approximately

$$\begin{aligned} &\frac{\sigma(\gamma + p \rightarrow Y + p)}{\sigma(\gamma + p \rightarrow J/\psi + p)} \\ &\approx \frac{\Gamma_Y M_Y^3 m_c^8}{\Gamma_{J/\psi} M_{J/\psi}^3 m_b^8} \frac{|\alpha_s(1+i\beta)x G_N(Q_{\text{eff}}^2[Y])|^2 C_Y(0)}{|\alpha_s(1+i\beta)x G_N(Q_{\text{eff}}^2[J/\psi])|^2 C_{J/\psi}(0)}. \end{aligned} \quad (53)$$

The first factor on the right-hand side of Eq. (53) is the dimensional estimate, and it yields a relative suppression of Y photoproduction of about 1:2000 if we set for the quark

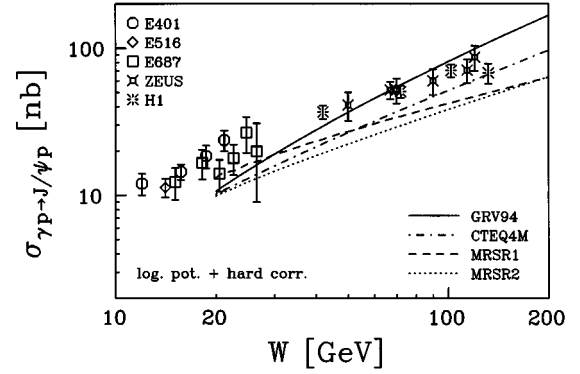


FIG. 11. The J/ψ photoproduction cross section for several recent parametrizations of the gluon density [34–36] in comparison with experimental data from E401 [37], E516 [38], E687 [39], ZEUS ’93 [40], and H1 [17].

masses $m_c=1.5$ GeV and $m_b=5.0$ GeV. The second term arises due to the so-called ‘‘rescaling of hard processes,’’ and it enhances the cross section ratio by a factor of about 3 for $x=10^{-3}$. The third term is connected to the wave function dependent effects, and it enhances the production ratio also by a factor of about 3. All together, the cross section for Y photoproduction is suppressed by approximately 1:200 as compared to J/ψ photoproduction for the same x . For the same W , an extra suppression factor $\approx (M_Y/M_{J/\psi})^{0.8} \approx 2.4$ is present. Note that the different Q^2 scale and higher twist effects [the ‘‘rescaling of hard processes’’ as well as the $\mathcal{C}(Q^2)$ correction] increase the relative yield that we predict by about an order of magnitude as compared to the naive dimensional estimate.

IV. THE J/ψ PHOTOPRODUCTION AND ELECTROPRODUCTION CROSS SECTION

In Fig. 11, we compare our predictions⁴ for the J/ψ photoproduction cross section with the data. We used a slope parameter of $B_{J/\psi} = 3.8$ GeV⁻², as measured by the H1 Collaboration [18], to calculate the total cross section from our predictions for the forward differential cross section at $t=0$, and the Fermi motion corrections and the ‘‘rescaling of hard processes’’ are accounted for. For the former, the charmonium potential of Ref. [5] was employed and the ‘‘hard physics’’ corrections, as outlined in Sec. III C, were taken into account. We furthermore replaced the quark pole mass with the running mass m_{run} from Eq. (38), and we set $x = (Q^2 + M_V^2)/W^2$. The formulas to obtain the forward differential cross section are given in Eqs. (50) and (51).

As can be seen from Fig. 11, the predictions of our PQCD calculation agree with the data within the uncertainties in the nucleon’s gluon density, and the energy dependence of the data is much better reproduced within the PQCD picture, where $\sigma \propto W^{0.7-0.8}$, than through the soft Pomeron model [1], where $\sigma \propto W^{0.32}$. A rough fit [18] to the data depicted in Fig. 11 yields $\sigma \propto W^{0.9}$.

⁴A respective FORTRAN program is available by request from koeopf@mps.ohio-state.edu or via the WWW at URL <http://www.physics.ohio-state.edu/~koeopf>

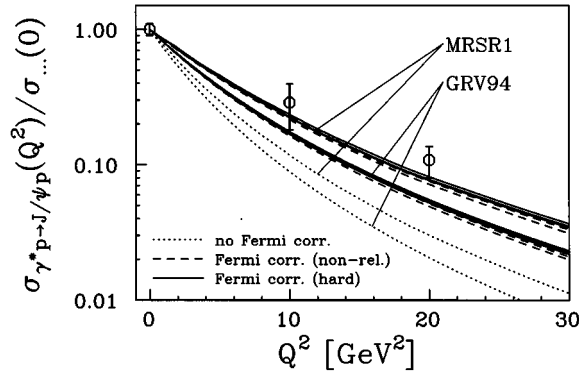


FIG. 12. The ratio of the J/ψ electroproduction to photoproduction cross section for two recent parametrizations of the gluon density [34,35] and for various potential models [5,6,9] in comparison with experimental data from H1 [17].

To investigate the Q^2 dependence of J/ψ production, we show in Fig. 12 the ratio of the electroproduction to photoproduction cross sections, i.e., we plot $\sigma_{\gamma^*+p \rightarrow J/\psi+p}(Q^2)/\sigma_{\gamma+p \rightarrow J/\psi+p}(Q^2=0)$ as a function of the virtuality of the photon. In particular, we compare a calculation where the Fermi motion corrections were left out (dotted lines), with an evaluation where the latter effects were included while either using just the nonrelativistic wave functions (dashed lines) or also accounting for the “hard physics” corrections (solid lines).

As can be seen from Fig. 12, the Fermi corrections are necessary to achieve agreement with the data. However, at this point, the quality of the data is not sufficient to distinguish between the various potential models or to decide whether the “hard physics” corrections which were imposed on those wave functions at small transverse interquark distances—see Sec. III C—lead to an improvement. This should change if the 1995 data, which have much better statistics, become available. The fact that we somewhat underestimate the J/ψ photoproduction cross section—see Fig. 11—and, at the same time, overestimate the Q^2 dependence of J/ψ electroproduction—see Fig. 12—suggests that our quark motion correction factor $\mathcal{C}(Q^2)$ of Eq. (51) is too small at $Q^2=0$ and it falls off too quickly at larger Q^2 . This implies that the wave functions which we use fall off too slowly in transverse momentum space and they are too steep as a function of the impact parameter b , i.e., the respective $\langle k_t^2 \rangle$ is too large.

V. THE ρ^0 ELECTROPRODUCTION CROSS SECTION

Although the main topic of this work is heavy meson photoproduction and electroproduction, we still consider an update of our predictions of Ref. [4] in regards to ρ^0 electroproduction warranted in light of the new data as well as theoretical developments in that realm. Currently, absolute cross sections for exclusive ρ -meson production are available from NMC [41], ZEUS [42], and H1 [18], and preliminary results exist from ZEUS from the 1994 run [19]. From our predictions for the forward differential cross section $d\sigma_{\gamma^*p \rightarrow \rho p}/dt|_{t=0}$ of Eq. (3), the total cross section was calculated using a slope parameter of $B_\rho=5 \text{ GeV}^{-2}$. This is

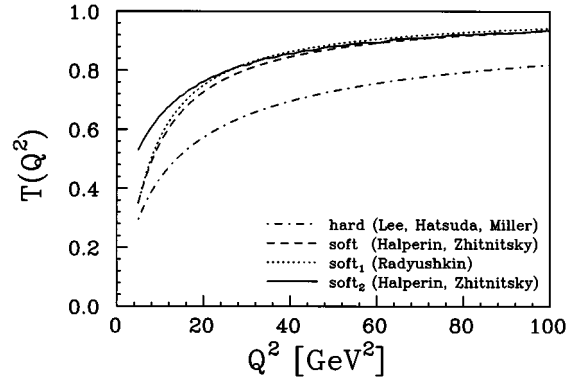


FIG. 13. The Fermi motion suppression factor $T(Q^2)$ of Eq. (4) for ρ^0 electroproduction for various ρ -meson wave functions from Refs. [43], [20], and [44].

consistent with the values given by the New Muon Collaboration (NMC) [41] ($4.6 \pm 0.8 \text{ GeV}^{-2}$) and ZEUS [42] ($5.1 \pm 1.2 \text{ GeV}^{-2}$) collaborations and slightly smaller than that obtained by H1 [18] ($7.0 \pm 0.8 \text{ GeV}^{-2}$).

To indicate separately the spread that arises from the different available gluon densities and the uncertainty that stems from the various proposed ρ -meson wave functions, the theoretical predictions are shown for two (extremal) gluon densities, Gluck-Reya-Vogt (GRV94) harmonic oscillator (HO) of Ref. [34] and Martin-Roberts-Stirling (MRSR2) of Ref. [35], and two different wave functions, termed “soft” and “hard.” The “soft” wave function refers to a $\phi_\rho(z, k_t) \propto \exp[-Ak_t^2/z(1-z)]$ with an average transverse quark momentum of $\langle k_t^2 \rangle = 0.18 \text{ GeV}^2$ as extracted from a QCD sum rule analysis by Halperin and Zhitnitsky [20], and the “hard” wave function corresponds to a $\phi_\rho(z, k_t) \propto z(1-z)[A/(k_t^2 + \mu^2)^2]$ obtained in another QCD sum rule analysis (for pions) by Lee, Hatsuda, and Miller [43]. For the latter, $\langle k_t^2 \rangle = 0.09 \text{ GeV}^2$. As outlined in detail in the above, the wave function enters through the Fermi motion suppression factor $T(Q^2)$ of Eq. (4). $T(Q^2)$ is depicted in Fig. 13 for various available ρ -meson wave functions: “hard” and “soft” were discussed in the above, “soft₁” refers to a duality wave function of the form $\Theta[s_0 - k_t^2/z(1-z)]$ with $\langle k_t^2 \rangle = 0.15 \text{ GeV}^2$ obtained in Ref. [44] and used for a similar analysis in [24], and “soft₂” labels a two-peak Gaussian favored in the analysis of Halperin and Zhitnitsky [20]. Note that the latter wave function seems quite extreme as it would correspond to a transverse spread of the $q\bar{q}$ component which is larger than the meson’s size.

The comparison of our predictions⁵ with the most recent experimental data is shown in Fig. 14. In the kinematic domain where our approach is expected to be applicable, $x \lesssim 0.01$ and/or $W \gtrsim 30 \text{ GeV}$, our predictions agree with the data within the spread through the various parametrizations for the gluon density and the uncertainty which stems from the vector meson’s wave function. Note, in particular, that as

⁵A respective FORTRAN program is available by request from koepf@mps.ohio-state.edu or via the WWW at URL <http://www.physics.ohio-state.edu/~koepf>

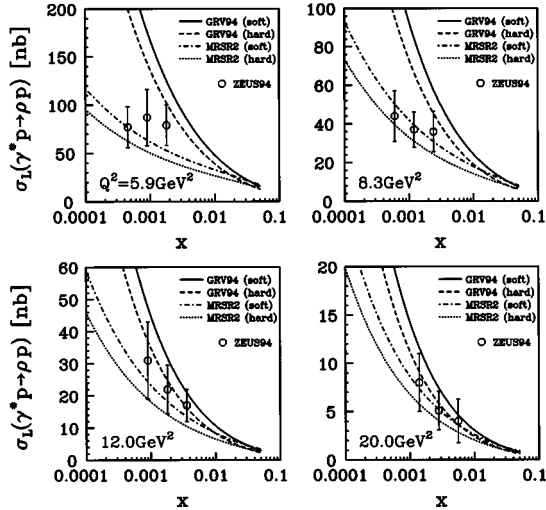


FIG. 14. The longitudinal ρ^0 electroproduction cross section $\sigma(\gamma_L^* + p \rightarrow \rho^0 + p)$ for two extremal parametrizations of the gluon density [34,35] and for two different ρ -meson wave functions in comparison with preliminary ZEUS data [19].

Q^2 increases the energy dependence of the preliminary ZEUS data [19] approaches more and more the hard physics limit, $\sigma \propto W^{0.7-0.8}$, which is very different from the soft Pomeron prediction [1], $\sigma \propto W^{0.22-0.32}$. This could indicate a transition from soft to hard physics in the Q^2 range depicted in Fig. 14.

There are two reasons why our predictions should not really reproduce the data very well at smaller Q^2 . Firstly smaller Q^2 correspond to larger transverse distances, and hence the PQCD approach outlined here loses some of its validity. Secondly, at very small x , the increase of these cross sections with energy is restricted by the unitarity of the S matrix, and even more stringent restrictions follow from the condition that the leading twist term should be significantly larger than the next to leading twist term [4]. The kinematical region where this limit becomes important moves to larger x for decreasing Q^2 . However, whether the softer energy dependence of the cross sections at the smaller Q^2 is really due to the unitarity limit slow down is unclear at the moment. Further work is in progress in that realm [45].

The Q^2 dependence of the cross section is commonly parametrized through a quantity α , where (for fixed W)

$$\sigma(\gamma^* + p \rightarrow \rho^0 + p) \propto Q^{-2\alpha}. \quad (54)$$

The various experiments yield $\alpha = 2.1 \pm 0.4$ [42], $\alpha = 2.4 \pm 0.3$ [19], and $\alpha = 2.5 \pm 0.5$ [18] at $\langle Q^2 \rangle \approx 12 \text{ GeV}^2$ and $\langle W \rangle \approx 80 \text{ GeV}$. Neglecting the Fermi motion corrections and the “rescaling of hard processes,” our theoretical predictions yield $\alpha \approx 3.3$ without the corrections, while we find $\alpha \approx 2.6$ if we take the quark motion and “rescaling of hard processes” into account. To evaluate the correction factor $T(Q^2)$ of Eq. (25), we again used the wave function $\phi_\rho(z, k_t) \propto \exp[-Ak_t^2/z(1-z)]$ with an average transverse quark momentum of $\langle k_t^2 \rangle = 0.18 \text{ GeV}^2$ as extracted from a QCD sum rule analysis [20]. Hence, our predictions agree with the measurements only if the Fermi motion corrections and the “rescaling of hard processes” are taken into account.

This underlines our claim [4] that the Q^2 dependence of those cross sections could eventually be used to probe the transverse momentum distributions within the produced vector mesons. However, at present, the data are still far too crude to extract conclusive information on this quantity. Note, furthermore, that our prediction refers to the Q^2 dependence of the longitudinal cross section σ_L while the experimental values listed in the above correspond to the Q^2 dependence of the total cross sections $\sigma = \sigma_T + \epsilon\sigma_L$.

VI. CONCLUSIONS

In this work, we focused the QCD analysis of Refs. [2] and [4] on heavy quarkonium (J/ψ and Y) photoproduction and electroproduction, and we extended the respective formalism, which in Refs. [2] and [4] was applied to the production of longitudinally polarized vector mesons only, to transverse polarizations as well.

For nonasymptotic momentum transfers, the respective hard amplitude is sensitive to the transverse momentum distribution in the $q\bar{q}$ light-cone wave function of the leading Fock component in the produced vector meson. This leads to a suppression of the asymptotic predictions, i.e., to an interplay between the quark(antiquark) momentum distribution in the vector meson and the Q^2 dependence of the corresponding cross section. We derived the respective expressions for the Fermi motion suppression factor, $T(Q^2)$ of Eqs. (7) and (25), and the relative enhancement of the transverse cross section, $R(Q^2)$ of Eqs. (6) and (26), to leading order in $1/(Q^2 + 4m^2)$.

The evaluation of these factors required a detailed study of the vector meson’s $q\bar{q}$ light-cone wave function. Motivated by the large value of the quark mass in heavy quarkonia, we started from conventional nonrelativistic potential models, which we critically examined and confronted with QCD expectations. In particular for the J/ψ meson, our numerical analysis yields a significant value for the high momentum component in the respective wave functions, visible in the lower part of Fig. 5, and a significant contribution of the “relativistic region” $v/c \geq 1$ to the integral $\int d^3k \phi_V(k)$, displayed in Fig. 6. This is in line with large relativistic corrections to the corresponding bound state equations [10]. These large relativistic effects question the feasibility of a description of heavy meson production in high energy processes based on a nonrelativistic ansatz. This is a very important result which should have consequences far beyond the scope of diffractive vector meson production, and it indicates that the J/ψ meson is not really a nonrelativistic system. We therefore designed an interpolation for the wave function of heavy quarkonia which smoothly matches the results obtained from nonrelativistic potential models with QCD predictions at short distances.

We then used the latter to evaluate the finite Q^2 corrections for diffractive J/ψ as well as Y production. We find fairly good agreement of our predictions with the J/ψ data, and we predict a measurable production of Y mesons at HERA—especially after a luminosity upgrade. We also update our comparison of longitudinal ρ^0 electroproduction with the data, putting special emphasis on preliminary ZEUS 1994 data [19] that became available only recently.

The discussion in this work affirms that hard diffractive

vector meson production is exactly calculable in QCD in the same sense as leading twist deep inelastic processes. This holds if only short distances contribute, which is the case for heavy flavors or production of longitudinally polarized ρ^0 at large Q^2 . The respective amplitude is expressed through the distribution of bare quarks in the vector meson and the gluon distribution in the target. This is qualitatively different from an application of the constituent quark model to these processes, as in Refs. [15] and [16]. On the other hand, it makes these processes an ideal laboratory to study the $q\bar{q}$ leading Fock state in vector mesons.

ACKNOWLEDGMENTS

We would like to thank E. Braaten, S. J. Brodsky, and R. J. Perry for a number of fruitful discussions. This work was supported in part by the Israel-U.S.A Binational Science Foundation under Grant No. 9200126, by the U.S. Department of Energy under Contract No. DE-FG02-93ER40771, and by the National Science Foundation under Grant Nos. PHY-9511923 and PHY-9258270. Two of us (L.F. and M.S.) would like to thank the DESY theory division for its hospitality during the time when part of this work was completed.

-
- [1] A. Donnachie and P. V. Landshoff, Phys. Lett. B **296**, 227 (1992).
- [2] S. J. Brodsky, L. L. Frankfurt, J. F. Gunion, A. H. Mueller, and M. Strikman, Phys. Rev. D **50**, 3134 (1994).
- [3] J. C. Collins, L. Frankfurt, and M. Strikman, Phys. Rev. D **56**, 2982 (1997).
- [4] L. L. Frankfurt, W. Koepf, and M. Strikman, Phys. Rev. D **54**, 3194 (1996).
- [5] C. Quigg and J. L. Rosner, Phys. Lett. **71B**, 153 (1977).
- [6] W. Buchmüller and S.-H. H. Tye, Phys. Rev. D **24**, 132 (1981).
- [7] A. Martin, Phys. Lett. **93B**, 338 (1980).
- [8] E. Eichten, K. Gottfried, T. Kinoshita, K. D. Lane, and T.-M. Yan, Phys. Rev. D **17**, 3090 (1978); **21**, 203 (1980); **21**, 313(E) (1980).
- [9] M. Brisudová and R. Perry, Phys. Rev. D **54**, 1831 (1996); M. Brisudová, R. Perry, and K. Wilson, Phys. Rev. Lett. **78**, 1127 (1997).
- [10] W.-Y. Keung and I. J. Muzinich, Phys. Rev. D **27**, 1518 (1983); H. Jung, D. Krücker, C. Greub, and D. Wyler, Z. Phys. C **60**, 721 (1993).
- [11] V. L. Chernyak and A. R. Zhitnitski, Phys. Rep. **112**, 173 (1984).
- [12] R. Barbieri *et al.*, Phys. Lett. **57B**, 455 (1975); Nucl. Phys. **B105**, 125 (1976); W. Celmaster, Phys. Rev. D **19**, 1517 (1979).
- [13] S. J. Brodsky and G. P. Lepage, *Perturbative Quantum Chromodynamics*, edited by A. H. Mueller (World Scientific, New York, 1989), pp. 39–240.
- [14] R. Karplus and A. Klein, Phys. Rev. **87**, 848 (1952); J. Schwinger, *Particles, Sources and Fields* (Addison-Wesley, New York, 1973), Vol. II.
- [15] M. G. Ryskin, Z. Phys. C **57**, 89 (1993).
- [16] M. G. Ryskin, R. G. Roberts, A. D. Martin, and E. M. Levin, Z. Phys. C **76**, 231 (1997).
- [17] S. Aid *et al.*, Nucl. Phys. **B472**, 3 (1996).
- [18] S. Aid *et al.*, Nucl. Phys. **B468**, 3 (1996).
- [19] ZEUS Collaboration, in *ICHEP '96*, Proceedings of the XXVIII International Conference on High Energy Physics, Warsaw, Poland, 1996, edited by Z. Ajduk and A. Wroblewski (World Scientific, Singapore, 1997).
- [20] I. Halperin and Zhitnitski, Phys. Rev. D **56**, 184 (1997).
- [21] L. Frankfurt, A. Freund, V. Guzey, and M. Strikman, hep-ph/9703449.
- [22] B. Blättel, G. Baym, L. L. Frankfurt, and M. Strikman, Phys. Rev. Lett. **70**, 896 (1993).
- [23] L. L. Frankfurt, G. A. Miller, and M. Strikman, Phys. Lett. B **304**, 1 (1993).
- [24] L. Frankfurt, A. Radyushkin, and M. Strikman, Phys. Rev. D **55**, 98 (1997).
- [25] A. V. Radyushkin, Phys. Lett. B **385**, 333 (1996).
- [26] P. Hoodbhoy, Phys. Rev. D **56**, 388 (1997).
- [27] A. H. Mueller, Nucl. Phys. **B335**, 115 (1990).
- [28] J. Bartels, C. Ewertz, H. Lotter, and M. Wusthoff, Phys. Lett. B **386**, 389 (1996).
- [29] J. Kogut and L. Susskind, Phys. Rep. **8**, 75 (1973).
- [30] H. Abramowicz, L. L. Frankfurt, and M. Strikman, in *Particle Physics, Astrophysics and Cosmology*, Proceedings of the SLAC Summer Institute, Stanford, California, 1994, edited by L. De Porcel and J. Chan (SLAC Report No. 484, Stanford, 1996), hep-ph/9503437.
- [31] L. Frankfurt, in Proceedings of the 3rd Workshop on Small-x and Diffractive Physics, Report No. ANL 26-29, 1996.
- [32] E. J. Eichten and C. Quigg, Phys. Rev. D **52**, 1726 (1995).
- [33] See, for instance, G. Sterman, *An Introduction to Quantum Field Theory* (Cambridge University Press, Cambridge England, 1993).
- [34] M. Glück, E. Reya, and A. Vogt, Z. Phys. C **67**, 433 (1995).
- [35] A. D. Martin, R. G. Roberts, and W. J. Stirling, Phys. Lett. B **387**, 419 (1996).
- [36] CTEQ Collaboration, H. L. Lai *et al.*, Phys. Rev. D **55**, 1280 (1997).
- [37] M. Binkley *et al.*, Phys. Rev. Lett. **48**, 73 (1982).
- [38] B. H. Denby *et al.*, Phys. Rev. Lett. **52**, 795 (1984).
- [39] P. L. Frabetti *et al.*, Phys. Lett. B **316**, 197 (1993).
- [40] M. Derrick *et al.*, Phys. Lett. B **350**, 120 (1995).
- [41] M. Arneodo *et al.*, Nucl. Phys. **B429**, 503 (1994).
- [42] M. Derrick *et al.*, Phys. Lett. B **356**, 601 (1995).
- [43] S. H. Lee, T. Hatsuda, and G. A. Miller, Phys. Rev. Lett. **72**, 2345 (1994).
- [44] A. V. Radyushkin, Acta Phys. Pol. B **26**, 2067 (1995).
- [45] L. Frankfurt, W. Koepf, and M. Strikman (work in progress).